Absorption of hydrophobic volatile organic compounds in renewable vegetable oils and esterified fatty acids: Determination of gas-liquid partitioning coefficients as a function of temperature

Paula Alejandra Lamprea Pineda[1], Joren Bruneel[1,2], Kristof Demeestere[1], Lisa Deraedt[1], Tex Goetschalckx[1], Herman Van Langenhove[1], Christophe Walgraeve[1]

[1]Research group Environmental Organic Chemistry and Technology (EnVOC), Department of Green Chemistry and Technology, Faculty of Bioscience Engineering, Ghent University, Coupure Links 653, 9000, Ghent Belgium

[2]Trevi nv, Air Division, Dulle-Grietlaan 17/1, 9050, Ghent, Belgium

Correspondence to: Christophe Walgraeve (Christophe.Walgraeve@UGent.be). Tel: +32 9 264 59 53, mobile: +32 0485 84 21 39

Co-authors: PaulaAlejandra.LampreaPineda@UGent.be, JBruneel@trevi-env.com, Kristof.Demeestere@UGent.be, Lisa.Deraedt@UGent.be, Tex.Goetschalckx@UGent.be, Herman.VanLangenhove@UGent.be, Christophe.Walgraeve@UGent.be.

Abstract

Air scrubbing is an effective technology to treat industrial polluted air loaded with VOCs. Water is the most widely used absorbent liquid, but when hydrophobic pollutants are treated, mass transfer between the gas phase and the liquid phase is limited. Therefore, organic solvents are an attractive option to improve the removal efficiency of hydrophobic VOCs. In this study, four esterified fatty acids (isopropyl isostearate, isopropyl laurate, isopropyl myristate and methyl oleate) and three vegetable oils (corn oil, peanut oil and sunflower oil) were evaluated as suitable absorption liquids for seven hydrophobic VOCs, i.e., toluene, m-xylene, ethylbenzene, butane, pentane, hexane and heptane. In addition, one synthetic silicone oil (polydimethylsiloxane) was used as a reference absorption liquid. Dimensionless gas-liquid partitioning coefficients (K_{GL}, $1.3x10^{-4}$ – $2.4x10^{-2}$) were determined as a function of temperature (25-50 °C) by an optimized dynamic absorption method (DynAb) using Selected-Ion Flow Tube Mass Spectrometry (SIFT-MS). Our experimental results show that, in all the absorption liquids tested, the lowest K_{GL} coefficients were obtained for m-xylene+ethylbenzene, followed by toluene. Isopropyl myristate was found to be the most efficient liquid to absorb the target VOCs, except for heptane where methyl oleate was better. Knowledge of the K_{GL} coefficients of hydrophobic VOCs in these absorption liquids is crucial for process optimization and modeling. Moreover, the effect of temperature is relevant for industrial applications where K_{GL} temperature dependence relations are often lacking. This study evaluates for the first time the use of three renewable vegetable oils and four esterified fatty acids as pure solvents for the absorption of industrially widely used hydrophobic VOCs, where except for toluene, very little or no research had been carried out.

Keywords: hydrophobic VOCs, gas-liquid partitioning coefficient, scrubbing, esterified fatty acid, oil, DynAb.

1. Introduction

The emission of volatile organic compounds (VOCs) into the atmosphere causes environmental and health risks [1,2]. These compounds are emitted in large quantities worldwide mainly by industrial facilities [3]. Hence, VOCs are subject to increasingly severe environmental restrictions that have driven the industry sectors to rely on control and emission reduction technologies in order to lower the exposure to VOCs (e.g., Directive 2010/75/EU [4] and 40 CFR, 59 [5]).

Scrubbing is one of the most widely applied air pollution control technologies because it is fast, safe and economically feasible [6,7]. It relies on the removal of VOCs from waste gas streams by contacting the contaminated air with a liquid solvent. The process takes place in a scrubber unit that is designed to provide good contact between both phases [8,9]. The rate and degree of removal depend among other factors on the affinity of the target compound to the liquid phase [10]. Water is the most widely used absorbent liquid, and it therefore limits the process to the removal of water-soluble VOCs. Therefore, since the removal of hydrophobic VOCs in scrubbers where water is used is not feasible [11], non-aqueous liquids are sought to be used as possible alternative absorption liquids [12,13].

An organic absorption liquid suitable for application in a scrubber should have (i) a high capacity to absorb VOCs, (ii) a low viscosity and high diffusion to improve the mass transfer of compounds from the gas to the liquid phase, (iii) a low vapor pressure to reduce losses of the absorption liquid by evaporation, (iv) no toxicity nor fire or explosion risks, (v) low or non-biodegradability to ensure regeneration, reduce solvent consumption and enable VOCs recovery; and (vi) a low cost [13–15]. As such, silicon oils, vegetable oils, fatty acid methyl esters (FAMEs), and bis(2-ethylhexyl) adipate (DEHA), have shown to be potential absorbent liquids [12,13]. Silicon oils and DEHA are widely used in industrial applications (e.g., as antifoam agents, lubricants, and plasticizers) [14], have low toxicity levels, and their large-scale production has led to low market prices [14,16]. In addition, the use of vegetable oils and FAMEs is more environmentally friendly compared to e.g., high boiling hydrocarbon mixtures [17], and previous studies have demonstrated their thermal regeneration (e.g., at 120 °C for high oleic sunflower oil) together with its minimal effect on subsequent absorption processes [19].

The affinity of hydrophobic compounds to the absorption liquid can be quantified by the equilibrium partitioning of the compound between the air and liquid phase (gas-liquid partitioning coefficient (-) or K_{GL}, Eq 1). The lower the K_{GL}, the higher the affinity of the compound for the liquid phase and therefore, the higher the removal of VOCs from the waste gas [18]. As an example, polydimethylsiloxane (PDMS), the most commercially available silicon oil, can reduce the K_{GL} of toluene (K_{GL} = 1.1x10^{-3} at 25 °C) up to 99.6% when compared to its air-water partitioning coefficient (K_{AW} = 2.7x10^{-1} at 25 °C) [19]. Similarly, experiments carried out by Hariz [15] with sunflower 5% (v/v) oil/water emulsions at room temperature (21 – 24 °C) led to K_{GL} values of toluene between 1.40x10^{-2} and 1.80x10^{-2}. Table 1 shows an overview of reported experimental K_{GL} coefficients of the hydrophobic VOCs of interest in this study for a broad selection of organic absorbents at different temperatures. The K_{AW} is included as a point of comparison to evaluate the absorption capacity of the organic liquid versus water. As seen in Table 1, the available data is mainly limited to organic liquids originating from petrochemical sources and to hydrophobic VOCs such as toluene and hexane.

$$K_{GL} = \frac{C_{gas}}{C_{liquid}} \ (-) \qquad \textit{Eq. 1}$$

This study aims to achieve a fundamental understanding and quantification of the partitioning behavior of seven hydrophobic VOCs commonly found in waste gases with four esterified fatty acids, three vegetable oils and one synthetic oil as absorption liquids. Toluene, m-xylene, ethylbenzene, butane, pentane, hexane and heptane were chosen as model VOCs due to their (i) common use and emission by various industrial activities (e.g., in the petrochemical industry from gasoline tanks and during oil storage) [20,21], (ii) broad difference in hydrophobicity and volatility (see Table S1) [22], and (iii) lack of studies especially for VOCs such as butane and pentane (see Table 1). Isopropyl isostearate, isopropyl laurate, isopropyl myristate, methyl oleate, peanut oil, corn oil, sunflower oil, and silicone oil (PDMS 20 cSt) were selected and evaluated as possible absorption liquids. These esterified fatty acids have not been explored until now as single-compound scrubbing liquids, and their commercial availability, large-scale production (lower costs), and broad use (e.g., cosmetic and pharmaceutical preparations and dietary supplements, among others) make them attractive for absorption applications. For the vegetable oils, and except for sunflower oil, only limited data on K_{GL} values are available. In addition, as PDMS 20 cSt is one of the most common liquids used for the absorption of hydrophobic VOCs (Table 1), it was selected as a reference absorption liquid. To compare the absorption capacity of the different liquids, K_{GL} values were determined by a dynamic absorption method (DynAb). This method was initially developed by Bruneel et al. [23] and, in this study, it was further optimized (e.g., liquid volume and addition of an antifoam material) for the set of compounds and absorption liquids selected. Moreover, the influence of temperature on the K_{GL} was evaluated and temperature dependence relations were established for the VOCs of interest and the best-performing absorbent liquids. The results obtained in this study are of great importance to improve the design and modeling of air treatment systems where organic liquids are used for absorption purposes.

Table 1. Experimentally determined gas-liquid partitioning coefficients (K_{GL}) of the VOCs of interest in this study, with different organic absorbents. K_{AW} is the air-to-water partitioning coefficient of the VOC at 25 °C unless otherwise stated [24]. *Compounds are arranged in order of increasing value of the target compound's K_{AW}. N.R. stands for not reported, DEHA for bis(2-ethylhexyl)adipate, DEHP for bis(2-ethylhexyl)phthalate, DIBP for diisobutyl phthalate, DIDP for diisodecyl phthalate, DIHP for diisoheptyl phthalate, DINP for diisononyl phthalate, PDMS for polydimethylsiloxane, and PEG for polyethylene glycol.*

VOC	K_{AW} (-)	Absorption liquid	K_{GL} (-)	T (°C)	Reference
		PEG 300	8.77×10^{-4}	25	[14]
		PEG 400	5.75×10^{-4}	25	[14]
		PEG 400	6.08×10^{-4}	25	[25]
		DIBP	3.61×10^{-4}	25	[14]
		DIDP	4.59×10^{-4}	25	[14]
		DEHA	3.02×10^{-4}	25	[14]
		DEHA	3.54×10^{-4}	25	[25]
		DEHA	5.65×10^{-4}	25	[26]
		DEHA	3.35×10^{-4}	20	[13]
		DIHP	4.09×10^{-4}	25	[14]
		DIHP	2.74×10^{-4}	18.5	[25]
		DEHP	2.74×10^{-4}	18.5	[25]
		DINP	3.13×10^{-4}	18.5	[25]
		Hexadecane	1.01×10^{-3}	25	[25]
		Oleyl alcohol (70 %)	6.11×10^{-4}	25	[25]
		Sunflower oil (30.2% oleic acid) [a, b]	1.58×10^{-2}	24	[15]
		Sunflower oil (30.2% oleic acid) [a, b]	1.80×10^{-2}	23	[15]
		Sunflower oil (30.2% oleic acid) [a, b]	1.70×10^{-2}	20.8	[15]
		Sunflower oil (86.3% oleic acid) [a, c]	1.52×10^{-2}	24	[15]
		Sunflower oil (86.3% oleic acid) [a, c]	1.40×10^{-2}	23.7	[15]
Toluene		Sunflower oil (86.3% oleic acid) [a, c]	1.48×10^{-2}	23.2	[15]
0.27		PDMS 5 cSt	2.06×10^{-3}	25	[27]
		PDMS 5 cSt	1.09×10^{-3}	25	[19]
		PDMS 20 cSt	6.98×10^{-4}	25	[14]
		PDMS 20 cSt	1.25×10^{-3}	25	[19]
		PDMS 50 cSt	5.99×10^{-4}	20	[13]
		PDMS 50 cSt	1.17×10^{-3}	25	[19]
		PDMS 100 cSt	1.09×10^{-3}	25	[19]
		PDMS	7.39×10^{-4}	20	[28]
		PDMS	6.46×10^{-4}	25	[26]
		Mineral oil [d]	6.69×10^{-4}	N.R.	[29]
		Vegetal oil [e]	7.90×10^{-4}	N.R.	[29]
		Waste engine oil [f]	4.66×10^{-4}	N.R.	[29]
		1:1 V:M [g]	3.30×10^{-4}	N.R.	[29]
		1:2:3 V:M:W [h]	9.83×10^{-5}	N.R.	[29]
		1:3:2 V:M:W [h]	1.04×10^{-4}	N.R.	[29]
		2:1:3 V:M:W [h]	1.25×10^{-4}	N.R.	[29]
		2:3:1 V:M:W [h]	2.18×10^{-5}	N.R.	[29]
		3:1:2 V:M:W [h]	2.29×10^{-5}	N.R.	[29]
		3:2:1 V:M:W [h]	2.31×10^{-5}	N.R.	[29]
		DEHA	3.12×10^{-4}	20	[30]
		PDMS 50 cSt	5.58×10^{-4}	20	[30]
m-Xylene	0.29	PDMS 20 cSt	3.50×10^{-4}	23	[31]

Ethylbenzene	0.32	DHIP	1.04×10^{-4}	18.5	[32]
		DEHP	1.21×10^{-4}	18.5	[32]
		DINP	2.53×10^{-4}	35	[32]
		PDMS 20 cSt	4.20×10^{-4}	23	[31]
Hexane	73.6	Hexadecane	4.20×10^{-3}	30	[33]
		Tetradecane	2.60×10^{-3}	30	[33]
		Undecane	3.80×10^{-3}	30	[33]
		1-decanol	7.30×10^{-3}	30	[33]
		Diethyl sebacate	1.15×10^{-2}	30	[33]
		2-undecanone	5.00×10^{-3}	30	[33]
		PDMS 20 cSt	3.40×10^{-3}	30	[33]
		PDMS 20 cSt	4.40×10^{-3}	23	[31]
		DIHP	3.96×10^{-3}	18.5	[32]
		DEHP	4.91×10^{-3}	19	[32]
		DINP	4.32×10^{-3}	18.5	[32]
Heptane	81.7	PDMS 20 cSt	2.50×10^{-3}	23	[31]

[a]Oil/water emulsion at 5% by volume (v/v).
[b]Commercial sunflower oil with 30.2% oleic acid.
[c]High oleic sunflower oil (HOSO); 86.3% oleic acid.
[d]Mainly saturated naphthenic and linear alkanes obtained from Exxon Mobile, USA [29].
[e]Commercially available oil product composed of fatty acid glycerides and obtained from Arowana Company, China [29].
[f]Obtained from a local auto repair shop. It contains mainly alkanes and some additives (oxidation inhibitors and detergent dispersants) [29].
[g]Volumetric ratio of vegetal oil (V) to mineral oil (M).
[h]Volumetric ratio of vegetal oil (V) to mineral oil (M) to water oil (W).

2. Materials and methods

2.1 Experimental reagents

A certified gas cylinder (NIPPON GASES, Belgium) containing toluene, m-xylene, ethylbenzene, butane, pentane, hexane and heptane in nitrogen (N_2) was used. Each VOC was present at 50 ppm_v. The physical-chemical properties of these VOCs are listed in Table S1. Four esterified fatty acids, i.e., isopropyl isostearate, isopropyl laurate, isopropyl myristate and methyl oleate (industrial grade; Oleon, Belgium), three vegetable oils that are commercially available for domestic use, i.e., sunflower oil, corn oil and peanut oil, and one common silicon-based organic polymer, i.e., PDMS 20 cSt (VWR, Belgium) were evaluated as absorption liquids. The physical-chemical properties and average fatty acid composition of the oils of interest in this study are listed in Tables S2 and S3, respectively.

To avoid interferences in the measurements by impurities present in the absorption liquids, before each experiment, the liquids were stripped for 24 hours with a N_2 stream (30 sccm) at room temperature.

2.2 Experimental set-up – DynAb method

The K_{GL} coefficients were experimentally determined using the dynamic absorption (DynAb) method initially developed by Bruneel et al., [23]. The method consists of bubbling a gas stream containing a constant concentration of VOCs (17 ppm_v) and at a fixed flow rate (45 sccm) through a column with a known volume (0.1-5.0 mL) of absorption liquid. The VOCs undergo mass transfer from the gas phase into the liquid phase until equilibrium is reached. The gas flow concentration at the outlet of the bubble column is constantly monitored using Selected-Ion Flow Tube Mass Spectrometry (SIFT-MS). As a result, a typical breakthrough curve is obtained from which the partitioning coefficient can be calculated.

Figure 1 shows a schematic representation of the experimental setup, and a detailed description can be found in the supplementary material (Text S1). Briefly, the VOCs-loaded gas stream was made by diluting the mixture of VOCs from the gas cylinder. An additional N_2 stream was used to flush the lines and the bubble column before starting. The bubble column consisted of a glass vial (15 mL) with a conical base (Brand, Germany) in which the gas flow was introduced at the bottom through a small polyether ether ketone (PEEK) tube (outer diameter 1 mm). This resulted in the formation of small gas bubbles. However, to minimize the risk of liquid entering the SIFT-MS, a tube with a larger internal diameter was placed after the bubble column (Figure 1). Moreover, an anti-foam packing (polyethylene wire mesh pad, 0.55 g) was added in case of strong foaming of the absorption liquid. The whole setup was placed in a thermostatic cabinet (TC 135 S, Lovibond, Germany) to maintain a constant temperature (controllable in the range between 25-50 °C).

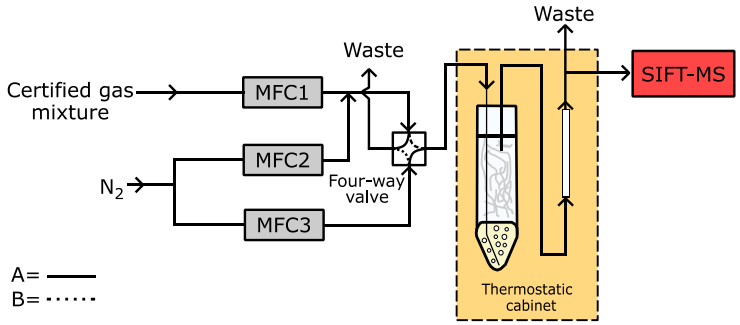

Figure 1. Schematic overview of the experimental set-up used to perform absorption experiments by the DynAb method. MFC stands for Mass Flow Controller and SIFT-MS for Selected-Ion Flow Tube Mass Spectrometry. Consider this figure together with the description in Text S1.

2.3 The DynAb experiment

A known volume (0.1-5.0 mL) of absorption liquid was pipetted into the bubble column and placed in the thermostatic cabinet. At the beginning of the experiment, the bubble column was flushed with a constant N_2 stream until all volatile impurities were removed and the temperature was constant. Afterward, the component stream was sent through the bubble column, and the VOCs were absorbed into the absorption liquid. The absorption process was monitored until equilibrium was reached (i.e., the incoming concentration equaled the outgoing concentration) by SIFT-MS. Moreover, to account for the possible adsorption of the target VOCs onto the glass column, tubing or anti-foam packing (see Section 3.1.2), a blank correction was performed with an empty vial (no liquid added) and keeping all the other parameters constant.

An initial step in the calculation of the partitioning coefficients is the normalization of the data. For this, the gas concentration measured from the beginning and the ingoing concentration that is equivalent to the maximal concentration or the outgoing concentration at equilibrium, are considered according to Eq. 2. In theory, equilibrium is only reached after infinite time, but for practical reasons, the measurements were stopped when the outgoing concentration equaled the incoming concentration for at least five minutes.

$$C_{gas}^{norm} = \frac{C_{out}}{C_{in}} \cdot 100 \qquad \textit{Eq. 2}$$

By plotting the normalized gas concentration as a function of time, for both the liquid sample and the blank, Figure 2 is obtained. The area A between both breakthrough curves is proportional to the absorbed mass of the compound in the liquid phase. Thus, the partitioning coefficient can be determined using the calculated area, provided that both the gas flow rate (Q) and the liquid volume (V) are known (Eq. 3).

$$K_{GL} = \frac{C_{gas,in}^{norm}}{C_{liquid}^{norm}} = \frac{100}{\frac{Q\left[\int_{t_0}^{t_\infty}\left[100 - C_{gas,sample}^{norm}(t)\right]dt - \int_{t_0}^{t_\infty}\left[100 - C_{gas,blank}^{norm}(t)\right]dt\right]}{V}} = \frac{100}{\frac{Q\,A}{V}} \qquad \textit{Eq. 3}$$

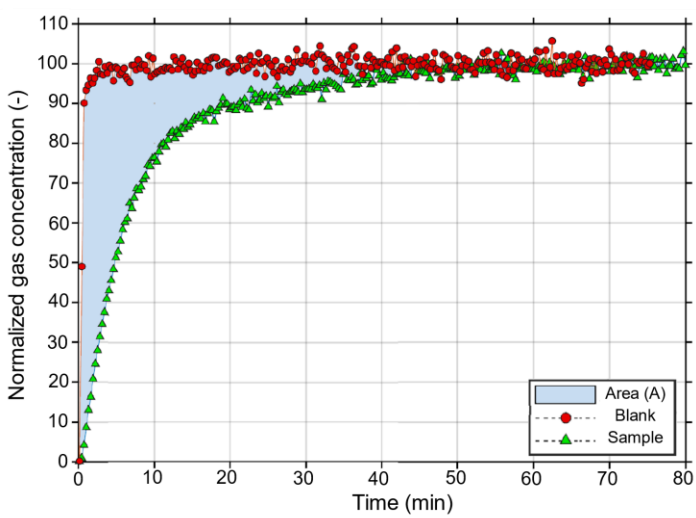

Figure 2. Typical breakthrough curves of the normalized gas concentration (C_{out}/C_{in}) as a function of time (min) in a bubble column without liquid (blank correction - red dots) and with absorption liquid (green triangles). The area (A) in blue between both curves is proportional to the absorbed mass of the VOC in the liquid phase.

2.4 Selected-Ion Flow Tube Mass Spectrometry (SIFT-MS)

The VOC concentrations in the gas phase were continuously measured throughout the whole experiment using a Voice 200 Syft technologies mass spectrometer (Interscience, Belgium). SIFT-MS is an online mass spectrometry technique that does not need analyte enrichment or sample preparation. SIFT-MS makes use of a soft ionization technique to generate precursor ions (most commonly H_3O^+, NO^+ and O_2^+). These ions react with trace components in the air but not with the major components of air (O_2 & N_2) itself. By using three different ions a larger specificity is obtained. In this way, a reaction fingerprint can be obtained for every component that reacts with at least one of the precursor ions [34]. For this study, the product ions (and their precursor ions) were selected based on (i) their branching ratio (BR – relative abundance = 100 %), (ii) reaction rate (≥ 1.7×10^{-9} molecules $cm^{-3}s^{-1}$), (iii) signal stability (Relative Standard Deviation (RSD) < 10 %) and (iv) interference between compounds. In this way, $C_7H_8^+$ [92]/NO^+ was selected for toluene, $C_8H_{10}^+$ [106]/NO^+ for ethylbenzene, $C_8H_{10}^+$ [106]/NO^+ for m-xylene, $C_4H_{10}^+$ [58]/O_2^+ for butane, $C_5H_{12}^+$ [72]/O_2^+ for pentane, $C_6H_{13}^+$ [85]/NO^+ for hexane, and $C_7H_{15}^+$ [99]/NO^+ for heptane. Because all product ions of ethylbenzene and m-xylene overlap (same mass-to-charge (m/z) ratio), the results are shown as m-xylene + ethylbenzene (in mixture) in the following sections.

2.5 K_{GL} experiments and effect of temperature

Initially, the volume of absorption liquid used for the DynAb method was optimized to determine reliable partitioning coefficients, within reasonable measurement times (see Section 3.1.1). Next, the effect of adding an anti-foaming packing material (polyethylene wire mesh pad, 0.55 g) was researched (see Section 3.1.2), and its influence on the K_{GL} values of the VOCs of interest was evaluated by carrying out experiments with and without anti-foaming packing material.

Finally, since the K_{GL} coefficients are temperature-dependent and from an application point of view, waste gas streams loaded with VOCs are often emitted at temperatures above ambient conditions, the determination of K_{GL} temperature dependence relations is of great importance. Therefore, K_{GL} measurements were conducted at different temperatures (25 - 50 °C).

The influence of the temperature on the K_{GL} was expressed by the Van 't Hoff equation according to Eq. 4.

$$Ln\ K_{GL} = -\frac{\Delta H_{G\rightarrow L}}{R \cdot T} + \frac{\Delta S_{G\rightarrow L}}{R} \qquad \textit{Eq. 4}$$

Where $\Delta H_{G\rightarrow L}$ and $\Delta S_{G\rightarrow L}$ are respectively the enthalpy and entropy change of the phase transfer from the gas to the liquid phase (J mol^{-1}), T is the temperature (K), and R is the universal gas constant (8.314 J mol^{-1} K^{-1}). A linear regression of the natural logarithm of K_{GL} as a function of the inverse of the temperature was performed and $\Delta H_{G\rightarrow L}$ was deduced from the slope, whilst $\Delta S_{G\rightarrow L}$ from the intercept.

3. Results and discussion

3.1 Optimization of the DynAb method

3.1.1 Absorption liquid volume

The area A between the two breakthrough curves (i.e., sample and blank curves) is proportional to the mass of VOC absorbed into the liquid after equilibrium (see Figure 2). Consequently, larger liquid volumes can absorb a larger mass of VOC before reaching equilibrium, and larger areas are thus obtained if all the other parameters remain constant. In general, compounds with low K_{GL} values that show a higher absorption capacity will retrieve higher areas compared to compounds with high K_{GL} values. Regardless of the type of

compound, a sufficiently large area is required to obtain a reliable calculation of the K_{GL}. According to this reasoning, enough liquid volume should be taken to obtain reproducible K_{GL} values. However, the time needed to determine the K_{GL} values is also dependent on the liquid volume used, and excessive amounts of liquid will translate into longer measurement times. Therefore, to determine the appropriate volume of absorption liquid needed to carry out the measurements, both the RSD and time of measurement were established as selection criteria for each VOC absorption measurement. As an example, an experiment using isopropyl myristate at different volumes (0.1-2.0 mL) shows for all the VOCs a clear improvement in RSD values when 2 mL was used compared to volumes below 1 mL (Table 2). The VOCs (e.g., heptane, toluene and xylene) with low K_{GL} values ($8.5x10^{-4}$ - $1.3x10^{-4}$) showed in most cases better RSDs (< 6%) in comparison to VOCs (e.g., butane, pentane) with higher K_{GL} values ($6.7x10^{-3}$ – $3.6x10^{-3}$), where an RSD up to 20% was obtained when an absorption liquid volume of 2 mL was used. Therefore, in order to lower the RSD of VOCs showing low absorption and to reduce the measuring time of strongly absorbing VOCs, absorption liquids between 0.1 – 5.0 mL were used for the following experiments.

Table 2. Average K_{GL} and corresponding RSD values for all VOCs in the different tested volumes of isopropyl myristate, with n the number of measurements. Time refers to the measurement time needed to obtain equilibrium partitioning.

VOC	Volume (mL)	K_{GL},avg (-)	RSD (%)	Time (hours)
Butane	< 1 mL (n=4)	$6.71x10^{-3}$	34	0.6 ~ 1.2
	2 mL (n=3)	$6.51x10^{-3}$	20	~ 2.3
Pentane	< 1 mL (n=4)	$3.58x10^{-3}$	34	0.6 ~ 1.2
	2 mL (n=3)	$4.36x10^{-3}$	20	~ 2.8
Hexane	< 1 mL (n=4)	$1.50x10^{-3}$	13	1 ~ 1.3
	2 mL (n=3)	$2.45x10^{-3}$	9	~ 2.1
Heptane	< 1 mL (n=4)	$5.99x10^{-4}$	6	1.2 ~ 2.2
	2 mL (n=2)	$8.47x10^{-4}$	1	~3.2
Toluene	< 1 mL (n=4)	$3.19x10^{-4}$	5	2.0 ~ 4.0
m-Xylene + Ethylbenzene	< 1 mL (n=4)	$1.27x10^{-4}$	6	2.1~ 6.8

3.1.2 Influence of anti-foam material

Among the set of absorption liquids selected in this study, the esterified fatty acids caused foaming under the conditions described in Section 2.2. Therefore, it was necessary to add an anti-foam material to minimize the risk of liquid entering the SIFT-MS. However, to determine if this material influenced the measured K_{GL} values (e.g., by adsorption), two blank measurements (i.e., empty vessel) were performed, one with anti-foam packing and one without it. This experiment showed (Table S4) that even though the anti-foam material adsorbs (up to 4 times larger areas than the areas without anti-foam packing) some of the incoming VOCs, such adsorption is considered here negligible compared to the absorption with the liquids used in this study (e.g., 15 to 35 times higher areas when isopropyl myristate is used).

3.2 Gas-liquid partitioning coefficients

The K_{GL} (-) coefficients obtained in this study range from $1.3x10^{-4}$ to $2.1x10^{-2}$ and – except for butane in silicone oil – they show good reproducibility (Table 3), with RSD values between 1% (heptane with isopropyl myristate or butane with corn oil) and 35% (hexane with methyl oleate). For any absorption liquid tested, the K_{GL} coefficients were always the lowest for m-xylene+ethylbenzene, followed by toluene. Contrary, butane and pentane in all cases showed the highest coefficients. Isopropyl myristate showed the highest absorption capacity for each compound, except for heptane which was absorbed to a larger extent in methyl oleate. Similar K_{GL} values were obtained for most VOCs in all three vegetable oils. Whereas the four esterified fatty acids showed K_{GL} values 5 to 12 times lower for toluene, m-xylene+ethylbenzene, hexane and heptane, compared to those obtained in silicone oil, the reference absorption liquid. In comparison to the K_{AW} of each VOC (0.27-81.7, Table 3), these results illustrate the potential use of these newly investigated renewable organic solvents for the absorption of hydrophobic VOCs. In particular, the K_{GL} of the studied VOCs decreased by a factor of $2x10^2$ (i.e., toluene in silicone oil) to $1x10^5$ (i.e., heptane in methyl oleate) when compared to water.

The low solubility of butane and pentane, and therefore high K_{GL} coefficients, in all the absorption liquids, compared to the other VOCs, can be explained by their high saturated vapor pressure. In fact, among the seven target VOCs, butane and pentane are the most volatile compounds (see Table S1), which makes it more difficult to trap them in the liquid phase. On the other hand, the low K_{GL} values observed for toluene and m-xylene+ethylbenzene can be explained by differences in polarity. Compared to the other VOCs, toluene, m-xylene and ethylbenzene are slightly polar VOCs (Table S1, dipole moment: 0.3 - 0.6 D), and the presence of e.g., a carboxylic acid group in the vegetable oils and an ester group in both the esterified fatty acids and the vegetable oils [35] can explain a higher solubility of both VOCs (polarizability of the π-electron cloud) in the absorption liquids. Moreover, as explained by Muzenda [36], the solubility of polar aromatic VOCs, such as toluene and m-xylene, decreases with an increase in the chain length of the ester solvent molecule. Thus, this explains why the K_{GL} coefficients of both compounds with isopropyl myristate and/or laurate are lower compared to isopropyl isostearate. On the other hand, the similarity in K_{GL} values obtained between the vegetable oils may be related to the fatty acid composition of each oil (Table S3). The biggest differences are observed mainly in the percentages of oleic and linoleic acid. In peanut oil, oleic acid dominates, while in the other two oils, linoleic acid is present in higher amounts. As indicated by Scheepers & Muzenda [37], an increase in the number of unsaturated bonds (oleic versus linoleic) results in a decreased solubility, which could explain the slightly lower K_{GL} values obtained with peanut oil.

To the best of our knowledge, there are no studies in which the four studied esterified fatty acids nor two of the vegetable oils (peanut and corn oil) have been evaluated as VOCs absorption liquids. Moreover, no data is available in the literature about K_{GL} of pentane or butane for any organic absorption liquid (see Table 1). The obtained K_{GL} values for toluene and hexane are in the same order of magnitude as those obtained when e.g., DIBP [14] and DEHA [14,25] at 25 °C, and tetradecane at 30 °C [33] are used, respectively. This indicates that DIBP, DEHA and tetradecane have similar absorption capacities for toluene and hexane compared to isopropyl isostearate, isopropyl laurate, isopropyl myristate and methyl oleate. In the case of toluene, Guillerm et al. [19] reported a similar K_{GL} value with silicone oil (PDMS 20 cSt) at 25 °C. On the other hand, the only value reported for heptane in literature is with PDMS 20 cSt [31], and it is almost 2 times higher than the one obtained in this study. The K_{GL} coefficient reported by the same author for ethylbenzene [31] is similar to the one obtained here for the mixture m-xylene+ethylbenzene.

Table 3. Experimentally determined dimensionless gas-liquid partitioning coefficients (K_{GL}) of the studied VOCs for the different absorption liquids, at 25-27°C. RSD stands for relative standard deviation and n for the number of repetitions. The air-water partitioning coefficient (K_{AW}) of each VOC was obtained from literature [24] *and is included as a reference to exemplify the solubility enhancement of the studied absorption liquids.*

	Toluene	**m-Xylene + Ethylbenzene**	**Butane**	**Pentane**	**Hexane**	**Heptane**
K_{AW}	0.27	m-xylene: 0.29 ethylbenzene: 0.32	38.8	51.1	73.6	81.7
Isopropyl isostearate (27 °C)						
K_{GL} (-)	3.6×10^{-4}	1.4×10^{-4}	1.8×10^{-2}	8.6×10^{-3}	2.8×10^{-3}	1.1×10^{-3}
RSD (%)	16	10	17	11	14	9
n	3	3	3	3	3	3
Isopropyl laurate (27 °C)						
K_{GL} (-)	3.2×10^{-4}	1.3×10^{-4}	1.1×10^{-2}	6.8×10^{-3}	2.7×10^{-3}	9.1×10^{-4}
RSD (%)	6	2	15	6	6	3
n	3	3	4	3	4	3
Isopropyl myristate (27 °C)						
K_{GL} (-)	3.2×10^{-4}	1.3×10^{-4}	6.5×10^{-3}	4.4×10^{-3}	2.4×10^{-3}	8.5×10^{-4}
RSD (%)	5	6	20	20	9	1
n	4	4	3	3	3	2
Methyl oleate (27 °C)						
K_{GL} (-)	3.4×10^{-4}	1.3×10^{-4}	7.5×10^{-3}	7.7×10^{-3}	3.2×10^{-3}	7.0×10^{-4}
RSD (%)	19	13	26	10	35	24
n	3	3	3	3	3	4
Silicone oil – PDMS 20 cSt (25 °C)						
K_{GL} (-)	1.2×10^{-3}	4.8×10^{-4}	1.6×10^{-2}	7.1×10^{-3}	3.9×10^{-3}	1.4×10^{-3}
RSD (%)	6	14	71	2	6	8
n	3	3	4	3	3	4
Sunflower oil (25 °C)						
K_{GL} (-)	4.6×10^{-4}	1.8×10^{-4}	2.1×10^{-2}	1.1×10^{-2}	4.4×10^{-3}	1.4×10^{-3}
RSD (%)	9	12	9	7	6	17
n	3	3	3	5	3	3
Corn oil (25 °C)						
K_{GL} (-)	4.4×10^{-4}	1.5×10^{-4}	2.0×10^{-2}	1.1×10^{-2}	3.8×10^{-3}	1.4×10^{-3}
RSD (%)	9	7	1	13	9	2
n	2	2	2	5	3	3
Peanut oil (25 °C)						
K_{GL} (-)	4.9×10^{-4}	2.0×10^{-4}	1.4×10^{-2}	6.4×10^{-3}	3.0×10^{-3}	1.1×10^{-3}
RSD (%)	6	12	22	10	17	5
n	3	3	3	3	3	3

3.2.1 Effect of carbon chain length on gas-liquid partitioning coefficients

The hydrophobicity of alkanes increases with increasing chain length. The addition of an extra carbon atom also increases the molecular weight, resulting in lower volatility. Hence, it is expected that longer alkanes have lower K_{GL} coefficients [35], indicating thus higher solubility in the non-polar absorption liquids. In fact, after toluene and m-xylene+ethylbenzene, the lowest K_{GL} coefficients in all absorption liquids were observed for heptane, followed by hexane, pentane and butane. In this case, the ester group of the esterified fatty acids and vegetable oils has little effect on the alkane-liquid (essentially non-polar) interaction compared to the aromatic-liquid interaction. Therefore, considering the octanol-water partitioning coefficient (Log (K_{OW})) of each VOC (see Table S1) as a measure of hydrophobicity, the more hydrophobic the VOC the higher its solubilization in the esterified fatty acids.

The influence of the carbon chain length on the K_{GL} of the linear alkanes is graphically presented in Figure 3 for the esterified fatty acids, and in Figure 4 for the vegetable and silicone oils. A linear relationship between the logarithm of the K_{GL} (Log (K_{GL})) and the carbon chain length of the alkanes ($R^2 > 0.95$, n = 4) is observed, except for methyl oleate. For the esterified fatty acids, a smaller slope – reflecting a higher absorption capacity – is obtained when isopropyl myristate is used instead of isopropyl isostearate (Figure 3). For the vegetable and silicone oils, similar slopes are obtained (Figure 4).

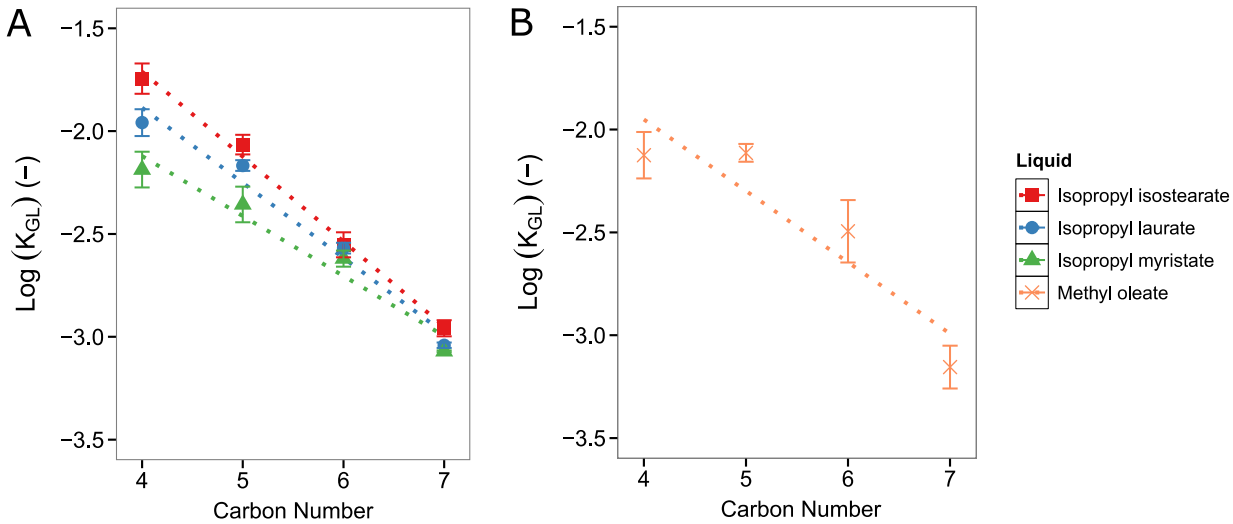

Figure 3. Logarithm of the partitioning coefficient (Log (K_{GL})) as a function of the carbon chain length of the linear alkanes at 27 °C, with the esterified fatty acids used as absorption liquid. (A) The following linear regressions are obtained: y = -0.41x+0.06 (R^2 = 0.99); y = -0.36x-0.43 (R^2 = 0.97); y = -0.29x+0.96 (R^2 = 0.95) when respectively isopropyl isostearate (red squares), isopropyl laurate (blue circles) and isopropyl myristate (green triangles) are used as absorption liquid. (B) The following linear regression is obtained when methyl oleate (orange crosses) is used as absorption liquid: y = -0.35x – 0.56 (R^2 = 0.84).

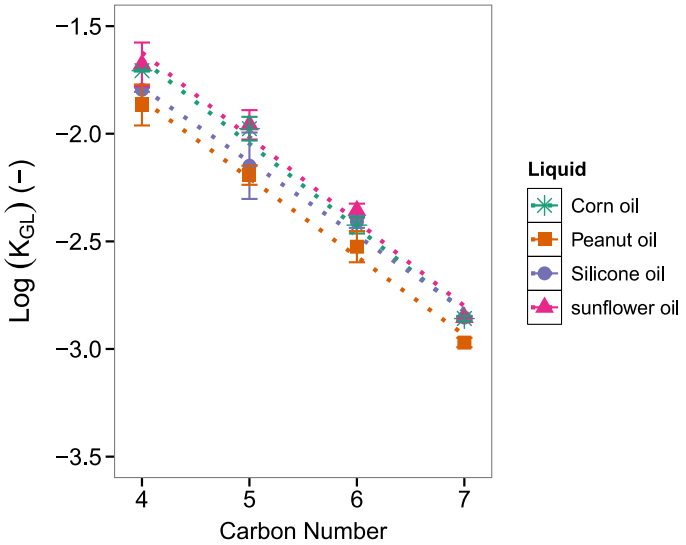

Figure 4. Logarithm of the partitioning coefficient (Log (K_{GL})) as a function of the carbon chain length of the linear alkanes at 25 °C, with the oils used as absorption liquid. The following linear regressions are obtained: y = -0.390x-0.096 (R^2 = 0.99); y = -0.364x-0.385 (R^2 = 0.99); y = -0.348x-0.386 (R^2 = 0.99); y = -0.386x-0.087 (R^2 = 0.99) when respectively corn oil (green asterisks), peanut oil (orange squares), silicone oil (purple circles) and sunflower oil (pink triangles) are used as absorption liquid.

When comparing the logarithm of the inverse of the K_{GL} (Log (1/K_{GL}) with the corresponding logarithm of the octanol-air partitioning coefficient (Log (K_{OA})) for all VOCs (Figures 5 and 6), it seems that Log (K_{OA}) can serve as a first predictor for the Log (1/K_{GL}) of hexane, heptane, toluene and m-xylene+ethylbenzene in the esterified fatty acids and vegetable oils. Indeed, in these cases, the amount of VOC that can be absorbed is underestimated by 1-9% depending on the absorption liquid and VOC. A more pronounced deviation from the 1:1 line is observed for butane (12-30%) and pentane (5-17%) (lowest Log (K_{OA}) values) in all the esterified fatty acids and peanut oil, and for toluene (14%) and m-xylene+ethylbenzene (14%) in silicon oil.

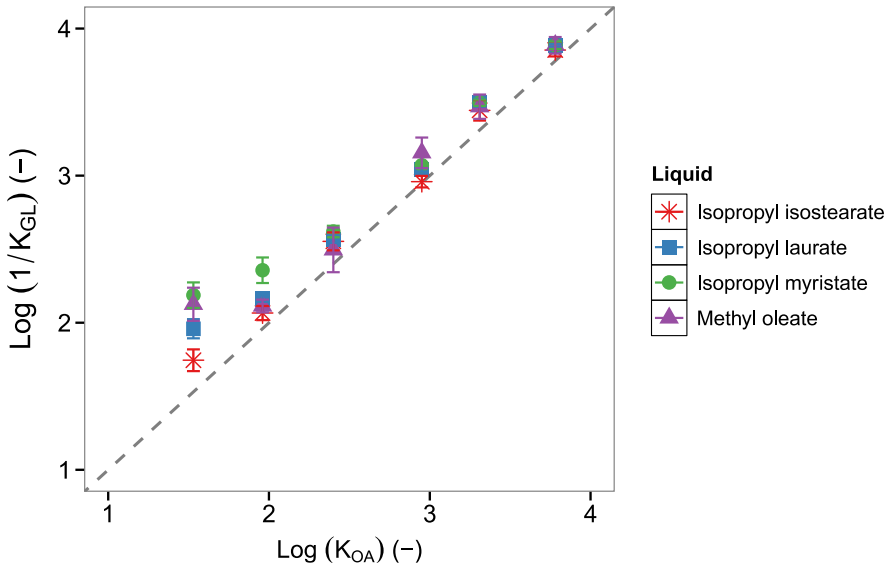

Figure 5. Logarithm of the inverse of the gas-liquid partitioning coefficient (Log (1/K_{GL}) (-)) of each VOC as a function of their corresponding logarithm of the octanol-air partitioning coefficient (Log (K_{OA}) (-)) (Table S1), at 27 °C for each esterified fatty acid.

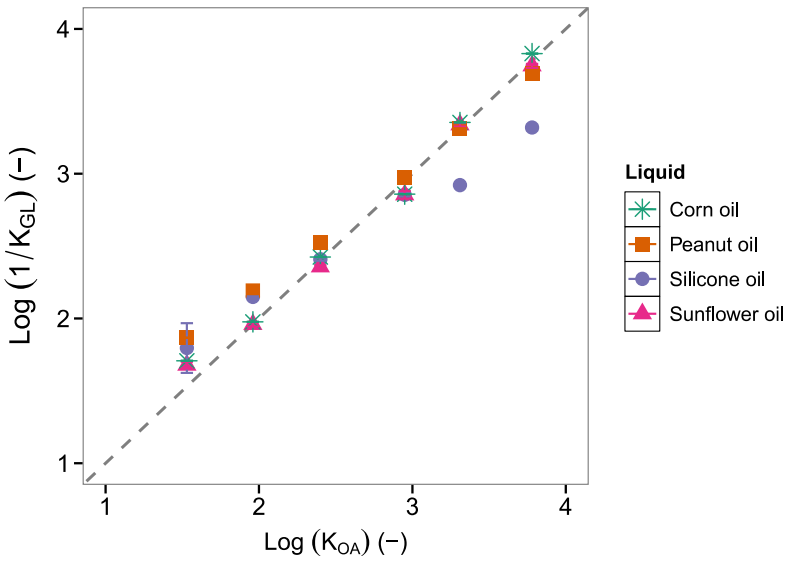

Figure 6. Logarithm of the inverse of the gas-liquid partitioning coefficient (Log (1/K_{GL}) (-)) of each VOC as a function of their corresponding logarithm of the octanol-air partitioning coefficient (Log (K_{OA}) (-)) (Table S1), at 25 °C for each oil.

3.2.2 Effect of temperature on gas-liquid partitioning coefficients

From an application point of view, the determination of K_{GL} values as a function of temperature is of paramount importance for air scrubbers. The efficiency of a scrubber decreases with an increase in temperature, which is later translated into a more frequent regeneration of the absorbent and thus, an increase in operating costs [15,28,38]. However, waste gas streams are typically released at temperatures above ambient conditions [39,40] and cooling such streams also has some associated costs. Therefore, the selection of a suitable absorbent liquid must consider among other things, its dependence on temperature.

The influence of the temperature on the K_{GL} values, as expressed by the Van 't Hoff equation, is depicted in Table 4 for the different VOCs and absorption liquids. These measurements were carried out only for the esterified fatty acids, except for methyl oleate. Among all the absorption liquids tested in this study, for most of the VOCs, lower K_{GL} coefficients were obtained with the esterified fatty acids, illustrating their higher absorption capacities compared to the oils. In addition, their lower viscosity compared to the oils (Table S5) makes them a promising option for future industrial applications. As indicated by Heymes et al. [14], low viscosity is an important criterion in the selection of a suitable liquid for the absorption of VOCs. Viscosity minimizes the thickness of the interface layer on the liquid side of absorption processes, which is translated into an improvement in diffusion kinetics and thus, mass transfer of compounds. In fact, the esterified fatty acids are 5.6 – 16 times less viscous than the vegetable oils, and even 2.2 - 5.3 times less viscous than the silicon oil selected in this study (Table S5). On the other hand, even though the absorption liquids were flushed with N_2, the increase in temperature for methyl oleate led to the release of impurities (e.g., hexanal, methyl heptanoate, etc.) that caused interferences in the SIFT measurements and made the measurements with this liquid unfeasible.

As expected, the solubility decreases with increasing temperature, and thus, higher K_{GL} coefficients were obtained at higher temperatures (Figure S1). Based on $\Delta H_{G\rightarrow L}$, the influence of the temperature on the K_{GL} for all the esterified fatty acids is the highest for m-xylene+ethylbenzene, followed by toluene, and the lowest for hexane. For heptane, toluene and m-xylene+ethylbenzene, $\Delta H_{G\rightarrow L}$ and $\Delta S_{G\rightarrow L}$ show the smallest difference between the three tested liquids. A more distinct difference, especially of $\Delta S_{G\rightarrow L}$, between the absorption liquids is noted for the lower alkanes, i.e., butane, pentane and hexane. The lower linear fit observed for these compounds (Table 4, R^2, and Figure S1) might be related to their volatility and its impact on the K_{GL}

measurements at higher temperatures. The increase in temperature resulted in higher K_{GL} values which, in turn, required larger absorption volumes. Even though RSD values below 20% were obtained in 92% of the cases for all compounds and absorption liquids, the higher volatility of e.g., butane and pentane and the lower absorption capacity of isopropyl isostearate compared to the other two esterifies acids (see Table 4), resulted in higher variability of the determined K_{GL} values at higher temperatures.

Table 4. Change in enthalpy ($\Delta H_{G \rightarrow L}$; kJ mol^{-1}) and entropy ($\Delta S_{G \rightarrow L}$; J mol^{-1}) ± standard errors (SE) of the phase transfer from the gas to the liquid phase for all VOCs and isopropyl isostearate, isopropyl laurate and isopropyl myristate as absorption liquids. Parameters are determined by Equation 1.1 after linear regression (n = 3).

	Butane	**Pentane**	**Hexane**	**Heptane**	**Toluene**	**m-Xylene + Ethylbenzene**
			Isopropyl isostearate			
$\Delta H_{G \rightarrow L}$(kJ mol^{-1})	-13.0±12.0	-23.5±10.6	-11.9±6.8	-26.5±8.9	-40.6±0.4	-41.8±4.8
$\Delta S_{G \rightarrow L}$(J mol^{-1})	8.7±38.8	39.8±34.2	-8.5±22.0	30.7±28.8	69.4±1.3	66.0±15.4
R^2	0.541	0.831	0.754	0.898	0.999	0.987
			Isopropyl laurate			
$\Delta H_{G \rightarrow L}$(kJ mol^{-1})	-24.8±7.3	-33.8±1.2	-22.1±6.0	-25.3±4.5	-39.6±1.9	-41.5±2.1
$\Delta S_{G \rightarrow L}$(J mol^{-1})	45.6±23.4	71.2±3.9	24.1±19.4	25.8±14.6	65.1±6.1	63.7±6.8
R^2	0.921	0.9990	0.931	0.969	0.998	0.997
			Isopropyl myristate			
$\Delta H_{G \rightarrow L}$(kJ mol^{-1})	-37.0±19.0	-24.7±30.5	-24.6±1.1	-28.3±1.2	-40.1±5.3	-40.6±0.5
$\Delta S_{G \rightarrow L}$(J mol^{-1})	82.3±61.0	38.9±98.0	31.9±3.6	35.5±3.9	66.3±16.9	60.7±1.7
R^2	0.791	0.396	0.998	0.998	0.983	0.999

4. Conclusions and recommendations

In this study, gas-liquid partitioning coefficients (K_{GL}) were determined for a broad range of hydrophobic VOCs (toluene, m-xylene+ethylbenzene, butane, pentane, hexane, heptane) using four esterified fatty acids (isopropyl isostearate, isopropyl laurate, isopropyl myristate and methyl oleate), three vegetable oils (corn oil, peanut oil and sunflower oil) and one synthetic oil (polydimethylsiloxane (PDMS)) as absorption liquids. The coefficients were experimentally measured with an optimized dynamic absorption method (DynAb), extending in this way its applicability towards a larger set of (foaming) absorption liquids. Moreover, the temperature dependency of the quilibrium partitioning was determined for the best performing absorption liquids and hydrophobic VOCs of interest to gain insight into the performance of future applications (e.g., in industrial scrubbers) where waste gas streams are typically released at temperatures above ambient conditions. Until now and except for toluene, very little or no research had been carried out for this set of VOCs (e.g., for pentane and butane removal) that are widely used and emitted by different industrial activities. This is the first study where single-compound esterified fatty acids (i.e., not applied in a mixture as e.g., in biodiesel) and renewable vegetable oils like peanut and corn oil, have been evaluated for absorption of hydrophobic VOCs.

All the studied absorption liquids were effective at reducing the K_{GL} values of the VOCs of interest compared to their K_{AW}. Butane was found to be the least absorbable compound, contrary to toluene and m-xylene+ethylbenzene which showed the highest solubility in both the esterified fatty acids and oils. Based on the results obtained in this study, isopropyl myristate shows the highest absorption capacity for all VOCs (K_{GL}= 1.3x10^{-4} – 6.5x10^{-3}), whereas similar or about three times higher K_{GL} values were obtained for most VOCs with all three vegetable oils (K_{GL}= 1.5x10^{-4} – 2.1x10^{-2}). The solubility of the VOCs decreased with increasing temperature, according to the Van 't Hoff equation, with hexane being the least affected by changes in temperature.

In future studies, it is recommended to evaluate the applicability and performance of the studied organic absorption liquids in industrial waste gas scrubbers and to further support the selection of the most optimal absorption liquid by economic and environmental considerations, such as the cost of the liquid, its regeneration and reuse, its storage and disposal, and its impact on e.g., food production and consumption. The latter is of particular relevance for the vegetable oils, which are nowadays used in food and for cooking.

5. Declaration of competing interests

The authors declare that they have no conflict (personal and/or financial) of interest.

6. CRediT authorship contribution statement

Paula Lamprea: Writing-original draft preparation, Data curation, Visualization and Supervision. Joren Bruneel: Conceptualization, Methodology, Supervision, Writing-Reviewing and Editing. Lisa Deraedt and Tex Goetschalckx: Visualization, Data curation. Kristof Demeestere, Herman Van Langenhove, Christophe Walgraeve: Conceptualization, Supervision, Writing-Reviewing and Editing, Resources.

7. Acknowledgments

This work was financially supported by Ghent University through a special research grant (BOFSTG2019005701) and the Flemish Agency for Innovation and Entrepreneurship (VLAIO, HBC.2018.0166).

8. Bibliography

[1] W. Wei, S. Cheng, G. Li, G. Wang, H. Wang, Characteristics of ozone and ozone precursors (VOCs and NOx) around a petroleum refinery in Beijing, China, J Environ Sci (China). 26 (2014) 332–342. https://doi.org/10.1016/S1001-0742(13)60412-X.

[2] H.R. Ghaffari, Z. Kamari, M.S. Hassanvand, M. Fazlzadeh, M. Heidari, Level of air BTEX in urban, rural and industrial regions of Bandar Abbas, Iran; indoor-outdoor relationships and probabilistic health risk assessment, Environ Res. 200 (2021). https://doi.org/10.1016/j.envres.2021.111745.

[3] H. Wang, S. Sun, L. Nie, Z. Zhang, W. Li, Z. Hao, A review of whole-process control of industrial volatile organic compounds in China, J Environ Sci (China). 123 (2023) 127–139. https://doi.org/10.1016/j.jes.2022.02.037.

[4] Directive 2010/75/EU of the European Parliament and the Council of 24 November 2010 on industrial emissions (integrated pollution prevention and control), L 334 (2010) 17–119.

[5] Environmental Protection Agency (EPA), PART 59—National volatile organic compound emission standards for consumer and commercial products, Environmental Protection Agency. (2016) 1–699. https://www.govinfo.gov/content/pkg/CFR-2016-title40-vol6/pdf/CFR-2016-title40-vol6-part59.pdf.

[6] L.J. Hsu, C.C. Lin, Binary VOCs absorption in a rotating packed bed with blade packings, J Environ Manage. 98 (2012) 175–182. https://doi.org/10.1016/j.jenvman.2011.11.011.

[7] X. Xiao, B. Yan, J. Fu, X. Xiao, Absorption and recovery of n-hexane in aqueous solutions of fluorocarbon surfactants, J Environ Sci (China). 37 (2015) 163–171. https://doi.org/10.1016/j.jes.2015.03.023.

[8] F.I. Khan, A.Kr. Ghoshal, Removal of volatile organic compounds from polluted air, Loss Prevention in the Process Industries. 13 (2000) 527–545. https://doi.org/https://doi.org/10.1016/S0950-4230(00)00007-3.

[9] T. Cao, Y. Zheng, H. Dong, Control of odor emissions from livestock farms: A review, Environ Res. 225 (2023) 115545. https://doi.org/10.1016/j.envres.2023.115545.

[10] F. Lalanne, L. Malhautier, J.C. Roux, J.L. Fanlo, Absorption of a mixture of volatile organic compounds (VOCs) in aqueous solutions of soluble cutting oil, Bioresour Technol. 99 (2008) 1699–1707. https://doi.org/10.1016/j.biortech.2007.04.006.

[11] X. Wang, R. Daniels, R.W. Baker, Recovery of VOCs from high-volume, low-VOC-concentration air streams, AIChE Journal. 47 (2001) 1094–1100. https://doi.org/10.1002/aic.690470516.

[12] M. Lhuissier, A. Couvert, A. Kane, A. Amrane, J.L. Audic, P.F. Biard, Volatile organic compounds absorption in a structured packing fed with waste oils: Experimental and modeling assessments, Chem Eng Sci. 238 (2021) 116598. https://doi.org/10.1016/j.ces.2021.116598.

[13] P.-F. Biard, A. Coudon, A. Couvert, S. Giraudet, A simple and timesaving method for the mass-transfer assessment of solvents used in physical absorption, Chemical Engineering Journal. 290 (2016) 302–311. https://doi.org/10.1016/j.cej.2016.01.046.

[14] F. Heymes, P. Manno-Demoustier, F. Charbit, J.L. Fanlo, P. Moulin, A new efficient absorption liquid to treat exhaust air loaded with toluene, Chemical Engineering Journal. 115 (2006) 225–231. https://doi.org/10.1016/j.cej.2005.10.011.

[15] R. Hariz, J.I. del Rio Sanz, C. Mercier, R. Valentin, N. Dietrich, Z. Mouloungui, G. Hébrard, Absorption of toluene by vegetable oil–water emulsion in scrubbing tower: Experiments and modeling, Chem Eng Sci. 157 (2017) 264–271. https://doi.org/10.1016/j.ces.2016.06.008.

[16] K. Bay, H. Wanko, J. Ulrich, Absorption of volatile organic compounds in biodiesel: Determination of infinite dilution activity coefficients by headspace gas chromatography, Chemical Engineering Research and Design. 84 (2006) 22–28. https://doi.org/10.1205/cherd.05050.

[17] H. Kim, T. Kim, N. Choi, B.H. Kim, S.W. Oh, I.H. Kim, Synthesis of diethylhexyl adipate by Candida antarctica lipase-catalyzed esterification, Process Biochemistry. 78 (2019) 58–62. https://doi.org/10.1016/j.procbio.2018.12.030.

[18] I. Wysocka, J. Gębicki, J. Namieśnik, Technologies for deodorization of malodorous gases, Environmental Science and Pollution Research. 26 (2019) 9409–9434. https://doi.org/10.1007/s11356-019-04195-1.

[19] M. Guillerm, A. Couvert, A. Amrane, É. Dumont, E. Norrant, N. Lesage, C. Juery, Characterization and selection of PDMS solvents for the absorption and biodegradation of hydrophobic VOCs, Journal of Chemical Technology and Biotechnology. 91 (2016) 1923–1927. https://doi.org/10.1002/jctb.4792.

[20] S. Saikomol, S. Thepanondh, W. Laowagul, Emission losses and dispersion of volatile organic compounds from tank farm of petroleum refinery complex, J Environ Health Sci Eng. 17 (2019) 561–570. https://doi.org/10.1007/s40201-019-00370-1.

[21] J.Y. Chin, S.A. Batterman, VOC composition of current motor vehicle fuels and vapors, and collinearity analyses for receptor modeling, Chemosphere. 86 (2012) 951–958. https://doi.org/10.1016/j.chemosphere.2011.11.017.

461 [22] C. Duan, H. Liao, K. Wang, Y. Ren, The research hotspots and trends of volatile organic compound
462 emissions from anthropogenic and natural sources: A systematic quantitative review, Environ Res.
463 216 (2023) 114386. https://doi.org/10.1016/j.envres.2022.114386.

464 [23] J. Bruneel, C. Walgraeve, K. Van Huffel, H. Van Langenhove, Determination of the gas-to-liquid
465 partitioning coefficients using a new dynamic absorption method (DynAb method), Chemical
466 Engineering Journal. 283 (2016) 544–552. https://doi.org/10.1016/j.cej.2015.07.053.

467 [24] P.H. Howard, W.M. Meylan, Handbook of physical properties of organic chemicals, CRC Press, Inc,
468 Boca Raton, The United States of America, 1997.

469 [25] M.D. Vuong, A. Couvert, C. Couriol, A. Amrane, P. Le Cloirec, C. Renner, Determination of the
470 Henry's constant and the mass transfer rate of VOCs in solvents, Chemical Engineering Journal. 150
471 (2009) 426–430. https://doi.org/10.1016/j.cej.2009.01.027.

472 [26] G. Darracq, A. Couvert, C. Couriol, A. Amrane, P. Le Cloirec, Integrated process for hydrophobic VOC
473 treatment-solvent choice, Canadian Journal of Chemical Engineering. 88 (2010) 655–660.
474 https://doi.org/10.1002/cjce.20325.

475 [27] E. Dumont, G. Darracq, A. Couvert, C. Couriol, A. Amrane, D. Thomas, Y. Andrès, P. Le Cloirec,
476 Determination of partition coefficients of three volatile organic compounds (dimethylsulphide,
477 dimethyldisulphide and toluene) in water/silicone oil mixtures, Chemical Engineering Journal. 162
478 (2010) 927–934. https://doi.org/10.1016/j.cej.2010.06.045.

479 [28] R. Tatin, L. Moura, N. Dietrich, S. Baig, G. Hébrard, Physical absorption of volatile organic
480 compounds by spraying emulsion in a spray tower: Experiments and modelling, Chemical
481 Engineering Research and Design. 104 (2015) 409–415.
482 https://doi.org/10.1016/j.cherd.2015.08.030.

483 [29] Z. Zhu, M. Yu, Z. Wu, Y. Yan, S. Li, Evaluation of the absorption performance of new compound
484 absorbents for toluene under extremely high load, Environmental Science and Pollution Research.
485 28 (2021) 52106–52123. https://doi.org/10.1007/s11356-021-14281-y/Published.

486 [30] P.F. Biard, A. Couvert, S. Giraudet, Volatile organic compounds absorption in packed column:
487 theoretical assessment of water, DEHA and PDMS 50 as absorbents, Journal of Industrial and
488 Engineering Chemistry. 59 (2018) 70–78. https://doi.org/10.1016/j.jiec.2017.10.008.

489 [31] M.J. Patel, S.C. Popat, M.A. Deshusses, Determination and correlation of the partition coefficients of
490 48 volatile organic and environmentally relevant compounds between air and silicone oil, Chemical
491 Engineering Journal. 310 (2017) 72–78. https://doi.org/10.1016/j.cej.2016.10.086.

492 [32] D. Bourgois, D. Thomas, J.L. Fanlo, J. Vanderschuren, Solubilities at high dilution of toluene,
493 ethylbenzene, 1,2,4-trimethylbenzene, and hexane in di-2-ethylhexyl, diisoheptyl, and diisononyl
494 phthalates, J Chem Eng Data. 51 (2006) 1212–1215. https://doi.org/10.1021/je050529h.

495 [33] S. Arriaga, R. Muñoz, S. Hernández, B. Guieysse, S. Revah, Gaseous hexane biodegradation by
496 Fusarium solani in two liquid phase packed-bed and stirred-tank bioreactors, Environ Sci Technol. 40
497 (2006) 2390–2395. https://doi.org/10.1021/es051512m.

498 [34] Syft Technologies Ltd, An overview of SIFT-MS, in: SIFT-MS Primer: An Introduction to the Chemistry
499 and Methodology of SIF-MS, Middleton, New Zeland, 2009: pp. 3–7.

500 [35] J.J. Scheepers, E. Muzenda, M. Belaid, Influence of Structure on Fatty Acid Ester- Alkane
501 Interactions, in: International Conference on Ecology, Agriculture and Chemical Engineering, 2012:
502 pp. 93–102.

503 [36] E. Muzenda, Aromatic compounds and ester polymeric solvents interactions, International Journal
504 of Chemical, Environmental & Biological Sciences. 2 (2014) 113–117.

505 [37] J.J. Scheepers, E. Muzenda, Alkenes – Ester polymeric solvents thermodynamic interactions - Part 1,
506 in: International Conference on Ecology, Agriculture and Chemical Engineering, 2012: pp. 229–233.

507 [38] N.F. Idris, N. Le-Minh, J.E. Hayes, R.M. Stuetz, Performance of wet scrubbers to remove VOCs from
508 rubber emissions, J Environ Manage. 305 (2022) 114426.
509 https://doi.org/10.1016/j.jenvman.2021.114426.

510 [39] H.L. Wang, L. Nie, J. Li, Y.F. Wang, G. Wang, J.H. Wang, Z.P. Hao, Characterization and assessment of
511 volatile organic compounds (VOCs) emissions from typical industries, Chinese Science Bulletin. 58
512 (2013) 724–730. https://doi.org/10.1007/s11434-012-5345-2.

513 [40] M. Luvsanjamba, B. Sercu, J. Van Peteghem, H. Van Langenhove, Long-term operation of a
514 thermophilic biotrickling filter for removal of dimethyl sulfide, Chemical Engineering Journal. 142
515 (2008) 248–255. https://doi.org/10.1016/j.cej.2007.11.038.

516